Simulation of pressure-induced polyamorphism in a chalcogenide glass GeSe$_2$

Murat Durandurdu and D. A. Drabold

Department of Physics and Astronomy, Ohio University, Athens, Ohio 45701-2979
(Received 17 September 2001; revised manuscript received 26 November 2001; published 4 March 2002)

The pressure-induced insulator-metal transition in amorphous GeSe$_2$ (a-GeSe$_2$) is studied using an *ab initio* constant pressure molecular-dynamic simulation. a-GeSe$_2$ transforms gradually to an amorphous metallic state under the application of pressure. The transition is reversible, and is associated with a gradual change from fourfold to sixfold Ge coordination, and from twofold to fourfold Se coordination. Pressure reduces the occurrence of chemical disorder up to 13 GPa. It is found that the optical gap decreases gradually, and the highly localized electronic and vibrational states of the glass at zero-pressure become extended with an increase of the pressure.

I. INTRODUCTION

Pressure-induced insulator-metal transitions have long attracted interest in the condensed-matter physics community. An area of recent emphasis is the amorphous-to-amorphous phase transition. For example a-Si,[1,2] a-Ge,[2] and H$_2$O (Ref. 4) show a first-order phase change from a low-density amorphous (LDA) to a high-density amorphous (HDA) phase while the transition proceeds gradually in SiO$_2$ (Refs. 3 and 5) and GeO$_2$.[6] In the case of amorphous and crystalline binary chalcogenide (AB_2, A=Ge, Si; B=S, Se) the pressure-induced phase transition is little understood. This is due to the challenge of constructing large realistic models, and the lack of good empirical potentials. In the present study, we perform a first-principles study to elucidate the mechanism of insulator-metal transition in amorphous GeSe$_2$ (a-GeSe$_2$). The material was intensively studied and thoroughly reviewed by Boolchand.[7]

For the crystal, three-dimensional $I\bar{4}2d$ (Refs. 8 and 9) and two-dimensional HgI$_2$ (Ref. 10) structures are reported at high pressure in chalcogenides. Recent experiments showed that crystalline GeSe$_2$ and GeS$_2$ transform to an amorphous state near 7 GPa at room temperature.[11] Shimada and Dachille[10] reported the production of a high-pressure form of a-GeSe$_2$, and noted that crystallization at temperatures below 573 K is inhibited. Also, they noted cristobalite and CdI$_2$ type compounds at about 3 and 7 GPa at 573–873 K. Grande *et al.*[9] reported that a-GeSe$_2$ compressed at 3 and 7.7 GPa (at 573 K) is partially crystallized. Prasad *et al.*[12] studied Ge$_x$Se$_{100-x}$ ($0 \leq x \leq 40$) glasses up to 14 GPa and temperatures 77–298 K, and observed a discontinuous glassy semiconductor to a crystalline metallic phase transition, contrary to observations by Shimada *et al.*[10] The high-pressure crystalline phases in a Ge$_x$Se$_{100-x}$ system do not correspond to any of the known GeSe$_2$ phases. Based on the experiments, it is argued that possible structural transitions in glassy GeSe$_2$, at high pressure and high temperature, could be similar to the ones in crystalline GeSe$_2$.[13]

In this paper, we present an *ab initio* constant pressure molecular dynamics (MD) study of a semiconductor-to-metal transition in a-GeSe$_2$, using a relatively large 216-atom realistic model. To our knowledge, this is the first direct MD simulation to model the pressure-induced phase transition in a-GeSe$_2$. We find that a-GeSe$_2$ undergoes a continuous transition to an amorphous metallic phase. The transition is reversible apparently because of the locality of the structural transformations. The coordination of Ge atoms changes gradually from a fourfold to a sixfold coordination while Se atoms transform from a twofold to a fourfold coordination. The initial compression causes a slight reduction of chemical disorder, while it leads to more topological disorder in the network. At high pressure, chainlike Se-Se clusters, emerge as seen in elemental Se. The intensity of the first sharp diffraction peak (FSDP) decreases smoothly, and its position shifts to a higher Q with increase of pressure. The optical gap decreases gradually with pressure. It is also found that highly localized electronic and vibrational states at zero pressure become extended with application of pressure.

II. METHODOLOGY

The simulation reported here is carried out in a large realistic 216-atom model of a-GeSe$_2$. The model is due to Cobb, Drabold, and Cappelletti, and is in uniform agreement with structural, vibrational, and optical measurements.[14] The model successfully produces the FSDP, which is in excellent agreement with the new experimental results[15] (see Refs. 14 and 16 for more details). The model was generated using a local orbital first-principles quantum-molecular-dynamics method which employs density-functional theory within the local density approximation and the Harris functional with hard norm-conserving pseudopotentials. The method is implemented entirely in real space. The short-range nonorthogonal single-ζ ($1s+3p$ per site) local orbital basis of compact slightly excited *fireball* orbitals of Sankey and Niklewski offered an accurate description of the chemistry with a significant computational advantage,[17] ideal for this complex system. The method was applied to form structural models of the surface of glassy GeSe$_2$,[16] liquid GeSe$_2$,[18] and a wide range of other amorphous materials.[19,20] The Hamiltonian successfully predicted a first-order pressure-induced phase transition in crystalline silicon (diamond to simple hexagonal), in amorphous silicon (amorphous to amorphous),[1] and in crystalline GaAs (zich-blende to *Cmcm* and *Imm2*).[21] Dynamical quenching under constant pressure
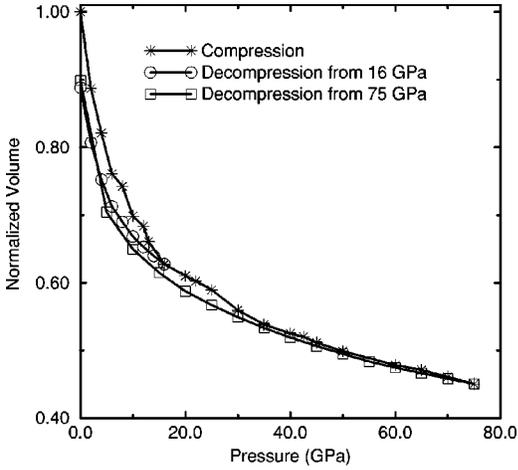
FIG. 1. The normalized volume of a-GeSe$_2$ changes smoothly with up to 12 GPa. After this pressure and several others, it shows slope changes. Upon a pressure release from 75 GPa, the path is reversed up to 30 GPa, and thereafter hysteresis is seen.

is performed to fully relax the system. Pressure is applied via the method of Parrinello and Rahman,[22] which enables the simulation cell to change volume and shape. The number of steps is chosen according to the criterion that the maximum force was smaller than 0.01 eV/Å. For some pressures, this required in excess of 7000 force calls. All the calculations used solely the Γ point to sample the Brillouin zone, which is reasonable for a cell with 216 atoms. A fictitious cell mass of 1.6×10^4 amu was found to be suitable for this simulation.

Once the equilibrium configuration under pressure is obtained, we compute the dynamical matrix, displacing every atom in the cell in three orthogonal directions (0.03 Å) and computing the resulting spring constants as second derivatives of the total energy of the system. Diagonalizing the dynamical matrix, we receive its eigenvectors and corresponding squared normal-mode frequencies ω^2, which enable us to carry out the full investigation of the vibrational behavior of the equilibrium configurations.

III. STRUCTURAL PROPERTIES UNDER PRESSURE

A. Pressure dependence of volume

We plot the pressure dependence of the relative volume in Fig. 1. The volume changes smoothly up to about 12 GPa, and then exhibits ''ripples'' at several pressures. At 12 GPa, $\sim 35.2\%$ atoms are involved in coordination changes, and the number of atoms suffering coordination modification increases to $\sim 51.9\%$ at 13 GPa. Since the volume drop at these pressures is relatively small, we interpret the pressure-induced phase change of a-GeSe$_2$ as a continuous transition, in stark contrast to results on a-Si.[1]

Our model reproduces the high-pressure form of the amorphous structure which is in excellent agreement with the experiment,[10] but, contrary to the study of Grande *et al.*[9] and Prasad *et al.*[12] It was shown that a-GeS$_2$ is crystallized at 873 K and densified at 543 K.[23] In a recent study, pressure-induced crystallization of vitreous ZnCl$_2$ was re-

ported at room temperature but, there is a transition to a HDA at low temperature.[24] The crystallization of an amorphous phase may be inhibited at low temperature and an amorphous-to-amorphous transition is favorable.

The pressure-volume curves on decompression at 16 and 75 GPa are given in Fig. 1. The path followed from 75 GPa is reversed up to 30 GPa. After this pressure the curve develops a hysteresis, as seen in the pressure release from 16 GPa. Such a hysteresis is perhaps expected after 12 GPa, because of the ripples seen in the pressure-volume curve. A decompression started at a different final pressure gives a very similar structure, albeit with small differences in density and coordination. In a contrast to SiO$_2$,[5] GeO$_2$,[6] H$_2$O,[4] and a-Si,[1] the amorphous-to-amorphous phase transition in a-GeSe$_2$ is reversible, as reported for a-As$_2$Te$_3$.[25]

B. Structural correlation

The effect of pressure on the FSDP was studied in many glasses. X-ray-diffraction patterns of GeS$_2$ glass,[26] x-ray diffraction of SiO$_2$,[3] pressure-densified SiO$_2$ glass,[27] and models[28] showed a decrease of the intensity of the FSDP, and a shift of its position into higher Q relative to the zero-pressure matrix. The densification of liquid GeSe$_2$ due to a temperature increase produces the same effect on the FSDP.[29] An experiment[3] also reported the appearance of a peak between the FSDP and the second peak in $S(Q)$ of SiO$_2$ under pressure.

The total $S(Q)$ and Faber-Ziman partial structure factors are depicted in Fig. 2. The intensity and position of $S(Q)$ exhibits dramatic changes at $Q<6$ Å^{-1} under pressure. The FSDP is weakened, and its position shifts to higher Q with the application of pressure. The result emphasizes an inverse correlation between the density (coordination) of the glassy materials and the FSDP. We also find the emergence of a peak at about 2 Å^{-1}. This peak is due to Ge-Ge correlations. The suppression of the FSDP and the emergence of the second peak suggest a change of the intermediate range order in the network.[3] Dramatic changes are observed in the second and third peaks: Although both peaks move to a higher Q, the intensity of the second peak increases while the third one decreases with pressure. All partials lend a contribution to the increase of the second peak, but Ge-Se correlations contribute predominantly. Generally the behavior of $S(Q)$ under pressure is in agreement with experiments on glassy systems.[3,26]

The total and partial real space pair distribution functions of a-GeSe$_2$ are given in Fig. 3. The position of the first peak shifts to a larger distance, and its intensity decreases with pressure, corresponding to the onset of the coordination change. The second peak position shifts to a lower distance with broadened distribution. The Ge-Se pair distribution function becomes quite uniform after the nearest-neighbor peak, except for a feature around 5.7 Å. With an increase of pressure, the position of the peak shifts to smaller distance with broadened distribution, which is parallel to how the
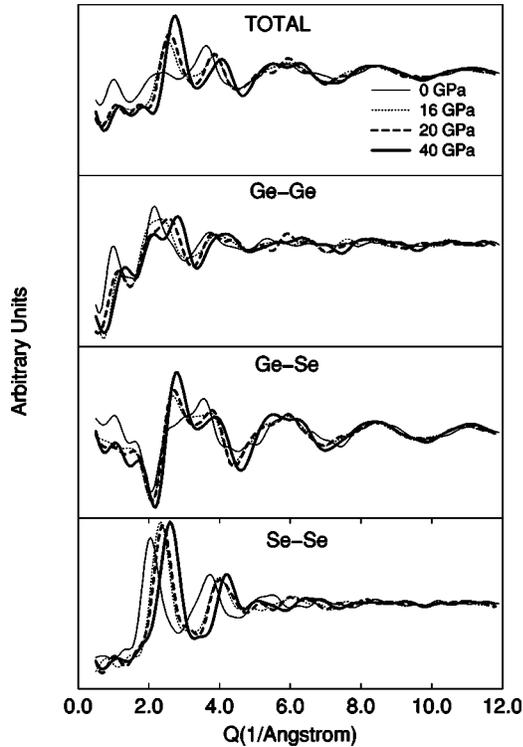
FIG. 2. The behavior of the total structure factor $S(Q)$ and Fiber-Ziman structure factors. The FSDP is suppressed, and its position shifts toward higher Q with increasing pressure. A new peak emerges at about 2 Å^{-1} which is mostly due to Ge-Ge correlation.

FIG. 3. The total and partial real-space pair distribution functions of a-GeSe$_2$.

FSDP changes with pressure. A new weak peak emerges around 3.2 Å in Ge-Se partial. The corresponding Q value for this distance is crudely estimated to be ~ 1.96 Å^{-1} using $r = 2\pi/|\mathbf{Q}|$, which is also in agreement with the appearance of a peak in $S(Q)$ at about 2 Å^{-1}. The nearest and second-nearest peaks in Se-Se correlations merge and make a broad peak around 2.8–3.2 Å. In addition, a second peak emerges at about 4.8–5.4 Å. The results suggest that Se atoms exhibit a comparatively large structural modification relative to Ge atoms. The Ge-Ge and Se-Se clusters at 65 GPa are given in Fig. 4. Surprisingly we find that Se atoms form chainlike clusters, as seen in pure Se, while Ge atoms form random clusters.

The bond angle distribution function is given in Fig. 5. We find dramatic changes in the position and intensity of the peak; the intensity of the peak decreases with the broad distribution, and its position shifts gradually to lower angles. We calculated the information entropy[30] of the bond angle distribution function at a given pressure using $S = -\Sigma_i P_i \ln P_i$, where P_i is the distribution of the bond angles. The entropy of the bond angle distribution function is a measure of how well defined the bond angles are at each pressure (large entropy, broad distribution). The pressure dependence of the entropy is depicted in Fig. 5. We find a very dramatic increase in the entropy up to 16 GPa, implying a fast structural change in the network. The curve then shows a change in slope, and the growth in S is slower. The utility of S for analyzing structural properties is under investigation.
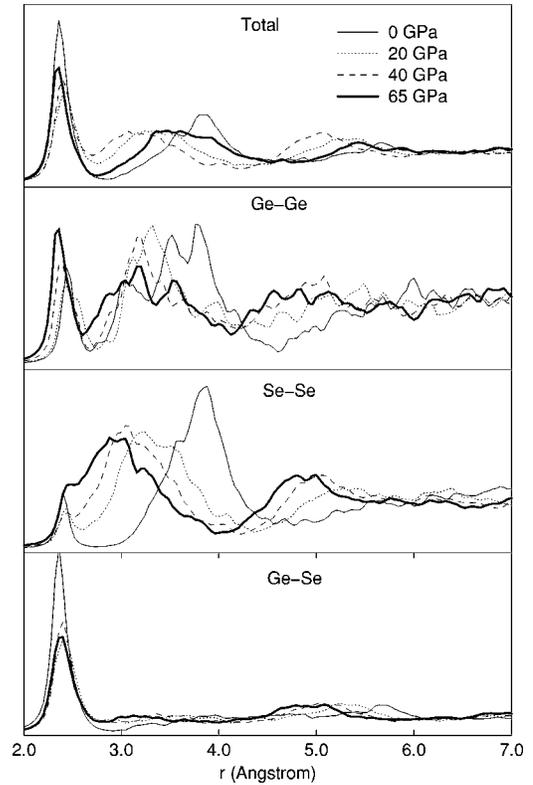
C. Topology and bonding under pressure

Table I presents structural properties of a-GeSe$_2$ at several pressures. We also plot the pressure dependence of structural properties in Fig. 6. The average coordination, which is defined from the first minimum of the total pair distribution function ($R_c = 2.70$–2.80 Å, depending on pressure) increases gradually up to 12 GPa. In a pressure range of 13–20 GPa, it shows a small abrupt increase at several pressures. Ge atoms transform gradually from fourfold to sixfold coordination while the average coordination of Se changes from twofold to fourfold. Either Ge or Se atoms involved in homopolar bond(s) have a tendency to form a more closely packed structure than those chemically ordered.

The average nearest-neighbor distance between atoms is given in Fig. 6. The average nearest-neighbor distance and the Ge-Se separation exhibit a small increase up to 12 GPa, and then both increase substantially in the pressure range of 12–16 GPa. Above 16 GPa, these separations do not show a significant modification but a small fluctuation. The increase of the neighbor distance is due to the formation of new bonds which are larger than the average. Pressure induces a large increase of the Se-Se separation. The large modification of the Se coordination is responsible for this behavior, yielding the occurrence of large Se-Se clusters in the network. On the other hand, the average Ge-Ge distance decreases, except for pressures at which ''ripples'' are observed in the pressure-volume curve.

One of the concerns in a-GeSe$_2$ is the quantity of chemical disorder, in particular the fraction of ''wrong'' (homopo-

(a)

(b)
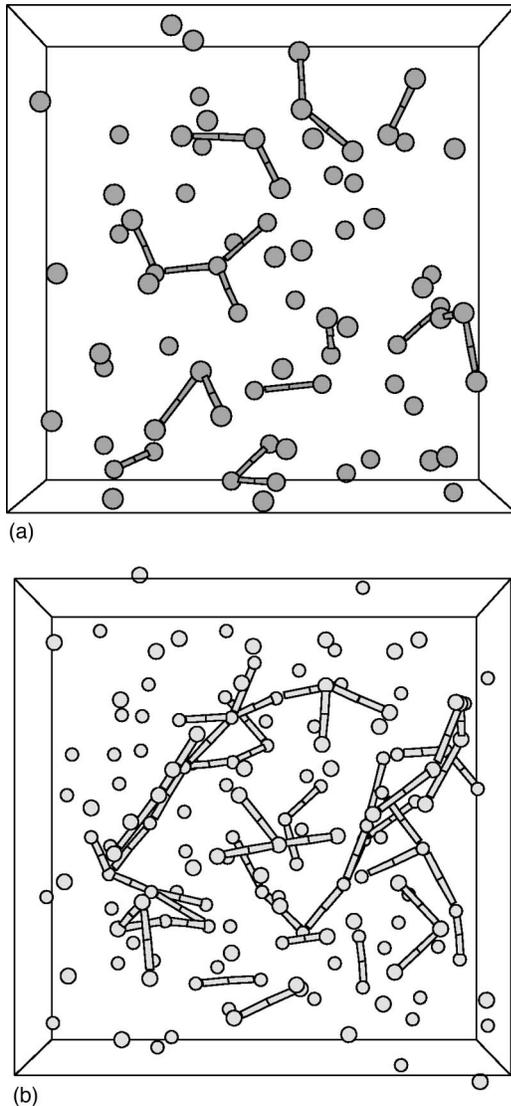
FIG. 4. Atomic configuration at 65 GPa. Ge (top) and Se (bottom) atoms are shown separately. Note the chainlike cluster of Se atoms.

lar) bonds between like atoms. The initial compression causes a slight reduction of wrong bonds in a-GeSe$_2$. In the pressure range of 12–20 GPa, there is a significant increase from $\sim 10.95\%$ to $\sim 17.11\%$ because of structural changes in the network. At 65 GPa, $\sim 28.48\%$ of the bonds are homopolar. The fraction of chemically disordered Ge and Se atoms as a function of pressure is given in Fig. 6. At zero pressure, 25% of Ge and Se atoms are involved in homopolar bonds, which is in close agreement with the value of 25(5)% Ge and 20(5)% Se (if only dimers are formed).[15] The fraction of Se atoms with wrong bonds does not change significantly up to 12 GPa, and then its behavior tracks that of the wrong bonds. The number of chemically disordered Ge atoms declines slightly in the presure range of 0–13 GPa. We find that some Ge-Ge homopolar bonds break under pressure, and the atom forms new bond(s) with decreasing or increasing coordination or sometimes without changing coordination depending on the local environment. In an experimental study

(a)

(b)
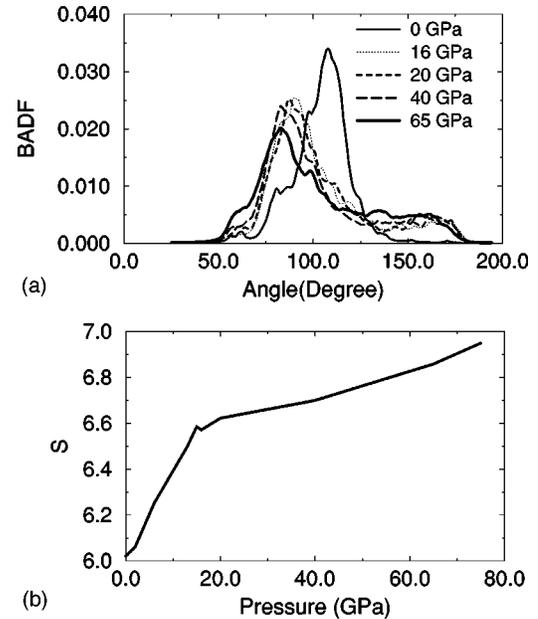
FIG. 5. (a) The bond angle distribution function (BADF). (b) The information entropy of the bond angle distribution function.

of pressure-induced amorphization of GeSe$_2$, it is reported that the Raman spectrum of the decompressed sample does not show the presence of the vibrational modes at about 180 cm^{-1}, indicating that pressure suppresses Ge-Ge bonding.[13] At 13 GPa, the number of Ge involved in homopolar bonding rises suddenly from $\sim 16.66\%$ to $\sim 26.28\%$, where the pressure-volume curve shows the first discontinuity. After 20 GPa, it increases gradually with pressure. In summary, pressure suppresses the occurrence of chemical disorder up to 13 GPa. At this pressure and thereafter, the system cannot resist an increase in chemical disorder. We note that while pressure reduces chemical disorder, it results in a softening of different parts of the network and in more topological disorder in the system, which leads to a gradual transformation to a HDA phase of a-GeSe$_2$.

D. Discussion

In oxide glasses and a-GeSe$_2$, the cation atoms transform gradually from fourfold to sixfold coordination, while the average coordination of the anion atoms is different; in SiO$_2$ and GeO$_2$, the anion atoms (O) transform from twofold to

TABLE I. Structural properties of a-GeSe$_2$ under pressure: average nearest-neighbor distance (ANND), average bond angle (ABA), and average coordination number (ACN) which is calculated from the first minimum of the PDF ($R_c = 2.70 - 2.80$ Å).

Pressure (GPa)	0	20	40	60	65
ANND (Å)	2.39	2.455	2.446	2.431	2.442
ABA	103.76°	102.87°	102.64°	102.51°	102.31°
ACN	2.68	3.46	4.04	4.40	4.84
ACN-Ge	3.86	4.83	5.52	6.08	6.10
ACN-Se	2.09	2.77	3.30	3.7	4.2
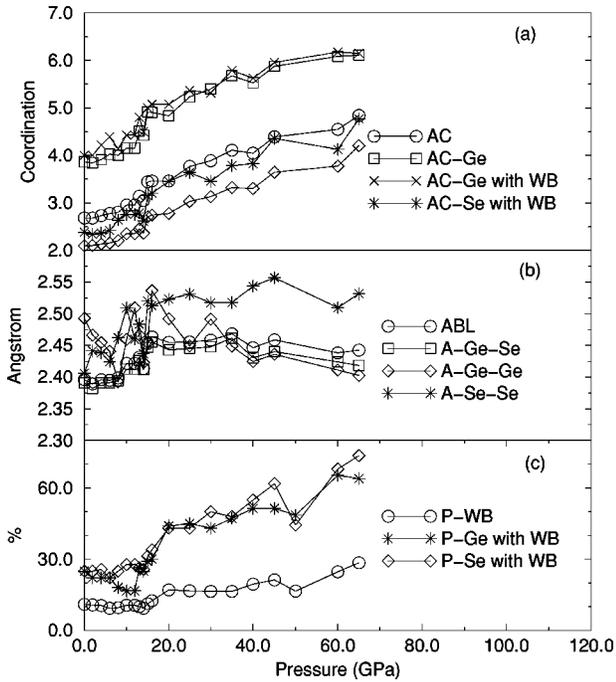
FIG. 6. Pressure dependence of structural properties of a-GeSe$_2$: (a) the average coordination (AC), the average coordination of Ge (AC-Ge), the average coordination of Se (AC-Se), the average coordination of Ge with wrong bond(s) (AC-Ge with WB), and the average coordination of Se with wrong bond(s) (AC-Se with WB). (b) The average bond length (ABL), the average Ge-Se separation (A-Ge-Se), the average Ge-Ge distance (A-Ge-Ge), and the average Se-Se separation (A-Se-Se). (c) The percentage of the total wrong bond (P-WB), the percentage of Ge atoms with wrong bond(s) (P-Ge with WB), and the percentage of Se atoms with wrong bond (P-Se with WB).

threefold coordination whereas the average coordination of Se in a-GeSe$_2$ change from twofold to fourfold. The existence of Se-Se clusters contribute to the increase of the co-ordination. This important distinction is due to the ionicity of the materials; the oxide glasses are far more ionic, and hence homopolar bonding is much disfavored.

Unlike elemental amorphous materials (selenium,[32] germanium,[2,33] and silicon[2]), the transition proceeds continuously in most amorphous compounds such as a-GaSb (Ref. 34) and a-GaAs.[31] Bond angle distributions seems to be a key signature of the behavior of a tetrahedral network under pressure.[34] Amorphous materials can be classified into two classes—a continuous transition class (mostly compounds) and a discontinuous transition class (mostly elemental)—based on their behavior under pressure. The similarity of these two classes is a structural disorder which causes a significant reduction in the transition pressure compared to their crystalline states. The difference is that the continuous transition class has chemical disorder in addition to structural disorder, and the importance of the chemical disorder is determined to a large extent by the ionicity (the more ionicity present, the more chemical order). To our knowledge, the effects of chemical disorder on pressure-induced phase transitions have not been studied or considered. The present study suggests that chemical disorder plays a very important
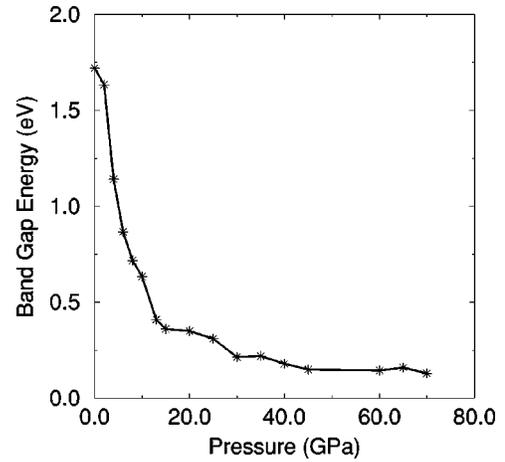
FIG. 7. Pressure dependence of the optical gap.

role in amorphous compounds. Since the formation of wrong bond(s) is unfavorable energetically (the penalty is small in a-GeSe$_2$), the application of pressure causes a suppression of the occurrence of chemical disorder, and simultaneously results in a decomposition of the different parts of the model. Therefore, we argue that not only structural disorder but chemical disorder need to be considered for a gradual transformation.

IV. ELECTRONIC STRUCTURE

Simulation enables us to study the electronic nature of a pressure-induced insulator-metal transition. It is found that both the conduction and valence tails shift to higher energies at low pressure. The shift of the valence tail dominates, producing a decrease of the band gap. Above 2 GPa, the conduction tails move to lower energies while the valence band continues to shift toward higher energies, implying a pronounced decrease of the band gap. A broadening of the bands under pressure is also observed. Figure 7 shows the pressure dependence of the optical gap in a-GeSe$_2$. The gap decreases nonlinearly with pressure. The decrease of the band gap is consistent with a previous report on a-GeSe$_2$.[35] In a pressure range of 2-16 GPa, the decrease is so pronounced because of the dramatic structural changes in the system.

Sakai and Fritzsche[25] pointed out that the decrease in the gap of chalcogenide semiconductors is associated with an increase of the dielectric constant, which tends to decrease the localization of the gap states and to promote metallic conduction at high pressure. In order to characterize the localization of electronic states through the transition, we define the Mulliken charge[36] $Q(n,E)$ for atom n associated with the eigenvalue E. This charge can then be used as a measure of the localization of a given state $Q_2(E) = N\Sigma_{n=1}^{N}Q(n,E)^2$, where N is the number of atoms in a supercell. For a uniformly extended state, $Q_2(E)$ is 1, while it is N for a state perfectly localized on a single atom. The localization of the electron states is shown in Fig. 8. Each peak in the figure represents an eigenvalue. The larger $Q_2(E)$ is for a state, the more localized the state is. At zero pressure, the top of the valence band is associated with
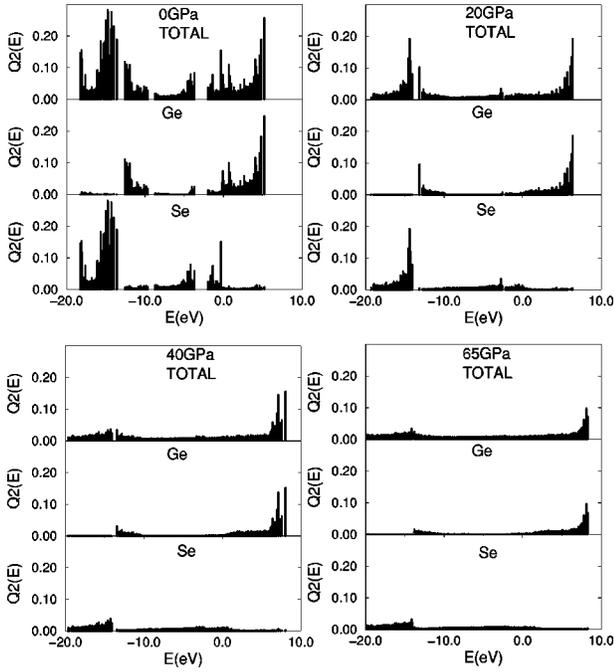
FIG. 8. Electronic eigenstates of a-GeSe$_2$ at several pressure. The position of the vertical bar represents the eigenvalues of the electronic eigenstates, and the height of the bars is the spatial localization $Q_2(E)$. Note the gradual delocalization of the states.

FIG. 9. Vibrational density of states on compression and decompression from 16 GPa.

threefold Ge atoms, twofold Se atoms forming Se dimers and onefold Se atoms, whereas the conduction-band edge is associated with threefold Se atoms to a large extent. The pressure-induced delocalization is due to the increasing number of overlapping orbitals, yielding a broadening of bands and a decrease of the gap. The localized states in the valence band at 20 GPa arise from threefold- and fourfold-coordinated Se atoms involved with at least two homopolar bonds. The result confirms our previous report[16] that Se-Se wrong bonds cause more localized states than the geometrically more defective structures. As the pressure increases, Se-related states become fully extended, while a few states associated with Ge atoms at the top of the conduction band are still localized (40 GPa). They are due to fivefold- and sixfold-coordinated Ge atoms with wrong bonds. At 65 GPa, all localized states are completely delocalized.

V. VIBRATIONAL DENSITY OF STATES

It is useful to predict the phonon modes for LDA GeSe$_2$ and HDA GeSe$_2$. The physical origin of the phase transition can be understood by examining the pressure-sensitive soft phonon modes. The vibrational density of states (VDOS) is given in Fig. 9. The bands shift to higher frequencies with pressure without softening modes, as reported in the Raman spectra of β-GeSe$_2$.[13] The same behavior was reported in theoretical[37] and experimental[38,39] studies of SiO$_2$. On the other hand, the modes of a-Si (Ref. 1) show very different behaviors compared to a-GeSe$_2$; in a-Si, the optical band shifts to higher frequencies up to a critical pressure, at which point the mode frequencies decrease abruptly whereas the acoustic modes soften at high pressure.

Particular attention was devoted to vibrational modes with energies around 200 cm^{-1}, with regard to the interpretation of features A_1 and A_{1c} modes. A_1 modes are in-phase breathing vibrations extended along corner-sharing GeSe$_4$ tetrahedral chain structures, and A_{1c} modes are breathinglike motions of Se about the edge-sharing GeSe$_4$ tetrahedra.[40,41] At low pressure, although the intensities of A_1 and A_{1c} change, their frequencies are not shifted, which is consistent with the Raman scattering study of a-GeSe$_2$ up to 2 GPa.[42] At 2 GPa, the intensity of A_1 decreases dramatically because of about 37.5% decrease of the corner-sharing tetrahedra. However, the intensity of A_{1c} modes increases and broadens, although we find about a 5% decrease in the concentration of clusters with edge-sharing GeSe$_4$ tetrahedra. Also, the intensity at about 180 cm^{-1}, which derives from the fact that the Ge-Ge bonding increases significantly even though the number of Ge atoms involved with homopolar bond(s) decreases at 2 GPa. The results suggest a strong correlation of the modes around 200 cm^{-1}. At 4 GPa, the feature around 200 cm^{-1} changes, and a strong peak at about 200 and 189 cm^{-1} merges because of the reconstruction.

At high pressures, the intensity of the bands decrease and the bands overlap. The VDOS of the zero-pressure model from decompression at 16 GPa is slightly different from that of the initial model. In the range of 0–150 cm^{-1}, no significant change is seen except for a small shift of the frequency. Dramatic changes are seen between about 150 and 240 cm^{-1}. The increase of the intensity of the peak at 180 cm^{-1} is due to the increase of Ge atoms with wrong bonds. The peaks around 200 cm^{-1} evolve a single peak with a broad distribution. In a Raman study of GeSe$_2$ under pressure, the spectrum of the sample obtained upon decompression is different from the melt-quenched amorphous samples, and it has been shown that very broad bands in the 150–300- cm^{-1}
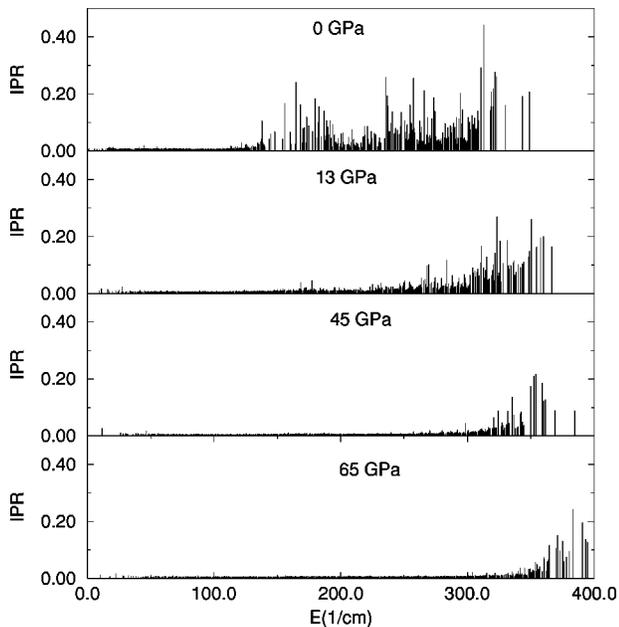
FIG. 10. Vibrational inverse participation ratio (IPR) of a-GeSe$_2$ under pressure. The highly localized modes at zero pressure are extended with the application of pressure.

region are well separated, and there is no low-wave-number shoulder feature in the 150–200-cm^{-1} region which is associated with the stretching vibration of the Ge-Ge bonds.[13] The spectrum obtained from pressure release presents results similar to those of the Raman study, except for the peak at around 180 cm^{-1}, which is probably due to the finite size of the simulation cell.

A convenient measure of the degree of the localization of the vibrational modes in an amorphous solid is the inverse participation ratio (IPR) equal to $N\Sigma_{j=1}^{N}(u_j \cdot u_j)^2[\Sigma_{j=1}^{N}(u_j.u_j)]^{-2}$. The calculated IPR of the models is depicted in Fig. 10. There are two types of the VDOS motion at zero pressure: (1) extended modes at frequencies less than 130 cm^{-1}, involving the motion of the entire tetrahedral units; and (2) more localized modes at frequencies higher

than 130 cm^{-1}, involving internal tetrahedral motion. The localized eigenmodes are extended with pressure. Similar change of the localized states has been observed in the theoretical study of SiO$_2$.[37]

VI. CONCLUSIONS

We have studied the pressure-induced insulator-metal transition in a-GeSe$_2$ using an *ab initio* constant pressure MD technique. a-GeSe$_2$ presents a reversible continuous phase transition into a metallic amorphous phase. The gradual changes of Ge (fourfold to sixfold) and Se (twofold to fourfold) coordinations is responsible for the amorphous-to-amorphous phase transition in a-GeSe$_2$. Pressure reduces the occurrence of chemical disorder, while simultaneously causing a softening of the different parts of the model and more structural disorder. We find an inverse correlation between the coordination of a-GeSe$_2$ and the FSDP and a reduction of the intermediate range order with an increase of pressure. Se-Se clusters at high pressure are chainlike, as seen in pure Se. Under pressure both localized electronic and vibrational states are delocalized.

These calculations strongly suggest that the pressure-induced structural changes are gradual in a-GeSe$_2$. It is possible that this conclusion could depend upon the finite size of the sample and or on limited sampling of possible conformations of the glass from using only one model. We suspect that these possibilities are remote, since the admittedly small (216 atom) model studied appears to have the characteristics of the real material compared to available experiments, and also because the changes seen in a-Si are *spectacularly* different (a first-order transition is observed). It is, nevertheless, worth repeating this type of study on a larger system.

ACKNOWLEDGMENTS

[1] M. Durandurdu and D. A. Drabold, Phys. Rev. B **64**, 014101 (2001).

[2] O. Shimomura, S. Minomura, N. Sakai, K. Asaumi, K. Tamura, J. Fukushima, and H. Endo, Philos. Mag. **29**, 547 (1974).

[3] C. Meade, R. J. Hemley, and H. K. Mao, Phys. Rev. Lett. **69**, 1387 (1992).

[4] O. Mishima, L. D. Calvert, and W. Whalley, Nature (London) **314**, 76 (1985).

[5] D. J. Lack, Phys. Rev. Lett. **84**, 4629 (2000); **80**, 5385 (1998).

[6] O. B. Tsiok, V. V. Brazhkin, A. G. Lyapin, and L. G. Khvostantsev, Phys. Rev. Lett. **80**, 999 (1998).

[7] See, for example, P. Boolchand, in *Insulating and Semiconducting Glasses*, edited by P. Boolchand (World Scientific, Singapore, 2000), p. 191.

[8] C. T. Prewitt and H. S. Young, Science **149**, 535 (1965).

[9] T. Grande, M. Ishii, M. Akaisi, S. Aasland, H. Fjellvag;, and S. Stølen, J. Solid State Chem. **145**, 167 (1999).

[10] M. Shimada and F. Dachille, Inorg. Chem. **16**, 2094 (1977).

[11] Z. V. Popovic, Z. Jaksic, Y. S. Raptis, and E. Anastassakis, Phys. Rev. B **57**, 3418 (1998); Z. V. Popovic, M. Holtz, R. Reimann, and K. Syassen, Phys. Status Solidi B **198**, 533 (1996).

[12] M. V. N. Prasad, A. Asokan, G. Parthasarathy, S. S. K. Titus, and E. S. R. Gropal, Phys. Chem. Glasses **34**, 199 (1993).

[13] A. Grezechnik, T. Grande, and S. Stølen, J. Solid State Chem. **141**, 248 (1998).

[14] M. Cobb, D. A. Drabold, and R. Cappelletti, Phys. Rev. B **54**, 12 162 (1996).

[15] I. Petri, P. S. Salmon, and H. E. Fischer, Phys. Rev. Lett. **84**, 2413 (2000).

[16] X. Zhang and D. A. Drabold, Phys. Rev. B **62**, 15 695 (2000).

[17] O. F. Sankey and D. J. Niklewski, Phys. Rev. B **40**, 3979 (1989).

[18] M. Cobb and D. A. Drabold, Phys. Rev. B **56**, 3054 (1997).

[19] M. Durandurdu, D. A. Drabold, and N. Mousseau, Phys. Rev. B **62**, 15 307 (2000).

[20] J. Li and D. A. Drabold, Phys. Rev. Lett. **85**, 2785 (2000).

[21] M. Durandurdu and D. A. Drabold (unpublished).

[22] M. Parrinello and A. Rahman, Phys. Rev. Lett. **45**, 1196 (1980).

[23] K. Miyauchi, J. Qiu, M. Shojiya, Y. Kawamoto, and N. Kitamura, J. Non-Cryst. Solids **279**, 186 (2001).

[24] C. H. Polsky, L. M. Matrinez, K. Leinenweber, M. A. VerHelst, C. A. Angell, and G. H. Wolf, Phys. Rev. B **61**, 5934 (2000).

[25] N. Sakai and H. Fritzsche, Phys. Rev. B **15**, 973 (1977).

[26] K. Tanaka, J. Non-Cryst. Solids **90**, 363 (1987).

[27] S. Susman, K. J. Volin, D. L. Price, M. Grimsditch, J. P. Rhino, R. K. Kalia, P. Vashishta, G. Gwanmesia, Y. Wang, and R. C. Liebermann, Phys. Rev. B **43**, 1194 (1991).

[28] S. R. Elliott, Phys. Rev. Lett. **67**, 711 (1991).

[29] I. Petri, P. S. Salmon, and W. S. Howells, J. Phys.: Condens. Matter **11**, 10 219 (1999).

[30] E. T. Jaynes, Phys. Rev. **106**, 620 (1957).

[31] S. Minomura, *High Pressure and Low-Temperature Physics* (Plenum, New York, 1978), p. 483.

[32] K. Tanaka, Phys. Rev. B **42**, 11 245 (1990).

[33] K. Tanaka, Phys. Rev. B **43**, 4302 (1991).

[34] V. A. Sidorov, V. V. Brazhkin, L. G. Khvostantsev, A. G. Lyapin, A. V. Sapelkin, and O. B. Tsiok, Phys. Rev. Lett. **73**, 3262 (1994).

[35] M. Kastner, Phys. Rev. B **7**, 5237 (1973).

[36] A. Szabo and N. S. Ostlund, *Modern Quantum Chemistry* (Dover, New York, 1996).

[37] W. Jin, R. K. Kalia, P. Vashishta, and J. P. Rino, Phys. Rev. Lett. **71**, 3146 (1993).

[38] P. McMillan, B. Piriou, and R. Couty, J. Chem. Phys. **81**, 4234 (1984).

[39] R. J. Hemley, H. K. Mao, P. M. Bell, and B. O. Mysen, Phys. Rev. Lett. **57**, 747 (1986).

[40] R. Cappelletti, M. Cobb, and D. A. Drabold, Phys. Rev. B **52**, 9133 (1995).

[41] S. Sugai, Phys. Rev. B **35**, 1345 (1987).

[42] Z. V. Popovic, M. Holtz, R. Reimann, and K. Syassen, Phys. Status Solidi B **198**, 337 (1996).